Open tubular liquid chromatography with thermal lens detection

ARTICLE *in* ANALYTICAL CHEMISTRY · JULY 1984

Impact Factor: 5.64 · DOI: 10.1021/ac00272a014

4 AUTHORS, INCLUDING:

John D Vargo
University of Iowa
28 PUBLICATIONS **602** CITATIONS
SEE PROFILE

Charles Kettler
Natoli Engineering
3 PUBLICATIONS **77** CITATIONS
SEE PROFILE

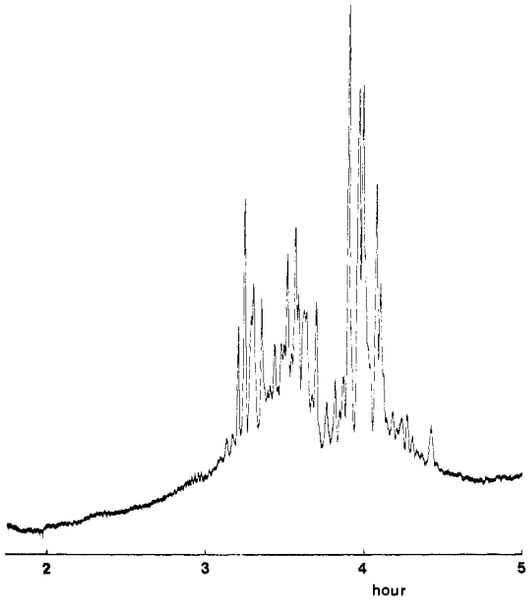

Figure 5. Separation of heavy oil, class A: column, 29 m × 42 μm; inlet pressure, 260 kg/cm^2.

aration at higher linear velocity is shown in Figure 4. N values for the last two peaks in Figure 4 are 68 000 and 53 000. The chromatogram of heavy oil, shown in Figure 5, looks nearly like that of the chromatogram obtained by capillary gas chromatography, although the former chromatogram still took a longer analysis period compared to that of the latter.

LITERATURE CITED

(1) Yang, F. J. *HRC CC, J. High Resolut. Chromatogr. Chromatogr. Commun.* **1983**, *6*, 348-358.
(2) Reese, C. E.; Scott, R. P. W. *J. Chromatogr. Sci.* **1980**, *18*, 479-486.
(3) Takeuchi, T.; Ishii, D. *J. Chromatogr.* **1981**, *218*, 199-208.
(4) Ishii, D.; Takeuchi, T. *J. Chromatogr.* **1983**, *255*, 349-358.
(5) Hirata, Y.; Jinno, K. *HRC CC, J. High Resolut. Chromatogr. Chromatogr. Commun.* **1983**, *6*, 196-199.
(6) Gluckman, J. C.; Hirose, A.; McGuffin, V. L.; Novotny, M. *Chromatographia* **1983**, *17*, 303-309.
(7) Tsuda, T.; Novotny, M. *Anal. Chem.* **1978**, *50*, 271-275.
(8) Hirata, Y.; Novotny, M.; Tsuda, T.; Ishii, D. *Anal. Chem.* **1979**, *51*, 1807-1809.
(9) Hirata, Y.; Novotny, M. *J. Chromatogr.* **1979**, *186*, 521-528.
(10) Novotny, M. *J. Chromatogr. Sci.* **1980**, *18*, 473-478.
(11) McGuffin, V. L.; Novotny, M. *Anal. Chem.* **1981**, *53*, 946-951.
(12) McGuffin, V. L.; Novotny, M. *J. Chromatogr.* **1981**, *218*, 179-187.
(13) McGuffin, V. L.; Novotny, M. *Anal. Chem.* **1983**, *55*, 2296-2302.
(14) Tsuda, T.; Tanaka, I.; Nakagawa, G. *J. Chromatogr.* **1982**, *239*, 507-513.
(15) McGuffin, V. L.; Novotny, M. *J. Chromatogr.* **1983**, *255*, 381-393.
(16) Tsuda, T.; Tsuboi, K.; Nakagawa, G. *J. Chromatogr.* **1981**, *214*, 283-290.
(17) Tijssen, R.; Bleumer, J. P. A.; Smit, A. C. C.; van Kreveld, M. E. *J. Chromatogr.* **1981**, *218*, 137-165.
(18) Krejci, M.; Tesarik, K.; Rusek, M.; Pajurek, J. *J. Chromatogr.* **1981**, *218*, 167-178.
(19) Jorgenson, J. W.; Guthrie, E. J. *J. Chromatogr.* **1983**, *255*, 335-348.
(20) Takeuchi, T.; Ishii, D. *J. Chromatogr.* **1983**, *279*, 439-448.
(21) Ishii, D.; Takeuchi, T. *J. Chromatogr. Sci.* **1980**, *18*, 462-472.
(22) Tsuda, T.; Nakagawa, G. *J. Chromatogr.* **1983**, *268*, 368-374.
(23) Knox, J. H.; Gilbert, M. T. *J. Chromatogr.* **1979**, *186*, 405-418.
(24) Knox, J. H. *J. Chromatogr. Sci.* **1980**, *18*, 453-461.
(25) Tsuda, T.; Ishii, D. The 22nd Symposium on Liquid Chromatography, Kyoto, Japan, Feb 16, 1979.
(26) Giddings, J. C. "Dynamics of Chromatograpy"; Marcel Dekker: New York, 1965.

RECEIVED for review December 6, 1983. Accepted February 27, 1984. Part of this paper was presented at the 7th International Symposium on Column Liquid Chromatography, Baden-Baden, F.R.G., May 2-6, 1983. This work was supported by a grand-in-aid from the Toyota Foundation (No. 82-1-III-031) and the Ministry of Education of Japan (No. 58390013).

Open Tubular Liquid Chromatography with Thermal Lens Detection

Michael J. Sepaniak,*[1] John D. Vargo,[2] Charles N. Kettler, and Michael P. Maskarinec

Department of Chemistry, University of Tennessee, Knoxville, Tennessee 37996-1600, and Analytical Chemistry Division, Oak Ridge National Laboratory, Oak Ridge, Tennessee 37830

Thermal lens detection is demonstrated for use in open tubular liquid chromatography. An argon ion laser beam is used to both create and probe thermal lenses formed in 100- and 200-μm flow cells. Base line noise levels of approximately 3 × 10^{-5} absorbance units are obtained. Chemically bonded, reverse-phase, open tubular columns with inner diameters of 20 μm are used to provide efficient separations of derivatized amines and nitroaniline mixtures. Laser fluorometric detection is employed to evaluate the columns and study the effect of flow cell design on chromatographic efficiency.

Several theoretical discussions regarding the relative merits of open tubular and packed liquid chromatography columns have appeared in the literature (*1-3*). Conclusions regarding which column type has the greater potential for high separating efficiency vary, depending largely on the author's choice of realistic operating parameters. However, there is general agreement that open tubular liquid chromatography (OTLC), using columns with inner diameters (i.d.) less than 10 μm and employing detectors with high sensitivity and low nanoliter volumes, will yield superior performance. Recent success in the chemical bonding of substrates to the inside surfaces of narrow-bore open tubular columns (*4, 5*) has greatly increased the analytical utility of OTLC. However, there still remains a need to develop detectors that satisfy the extremely low volume and high sensitivity requirements of OTLC.

Electrochemical (*6*), mass spectrometric (*7*), and spectrophotometric detection have been used in the development of OTLC. Novotny and McGuffin used flame photometric detection to monitor organophosphorus compounds separated by packed microcapillary columns (*8*). Commercial absorbance and fluorescence liquid chromatography detectors can be used in OTLC if a makeup flow is employed at the detector inlet (*9*). However, the large amount of sample dilution that occurs

[1] Author to whom correspondence should be addressed at the University of Tennessee.
[2] Present address: General Motors Research Laboratories, Analytical Chemistry Division, Warren, MI 48090-9055.

0003-2700/84/0356-1252$01.50/0

limits the value of that approach. Most of the reported research in OTLC has utilized absorbance or fluorescence detection, with the measurement being performed either on-column (*4*, *10*, *11*) or in miniaturized flow cells (*5*, *12*, *13*). Unfortunately, when absorbance or fluorescence detection is used in conjunction with extremely narrow-bore columns, short optical path lengths, large amounts of stray radiation, and poor light throughput can seriously limit detector performance. These problems should be less significant when a laser, with its high power and unique spatial properties, is employed as the radiation source. The volumes of focused laser beams are typically in the low nanoliter range (*14*). When used with on-column detection or with a suitable flow cell, laser-based spectrophotometric detectors should be capable of maintaining the high chromatographic efficiencies of extremely narrow-bore capillary columns.

The sensitivity of laser-excited fluorimetry makes that mode of detection desirable whenever the compounds of interest have reasonably large fluorescence quantum efficiencies or can be made to fluoresce through derivatization. The use of laser fluorometric detection in HPLC has been reviewed (*14*) and, more recently, its application to separations with microbore columns has been demonstrated (*15*).

Absorbance detection is much more versatile than fluorescence detection. However, the relatively poor sensitivity of the technique often necessitates the injection of sample quantities which overload OTLC columns (see below). Thermal lens calorimetry, a technique which relies on the formation of a refractive index gradient in a sample induced by the absorption of a laser beam, has been used to measure absorbances much lower than those that can be measured by the conventional absorbance technique (*16*, *17*). Thermal lens detection has been demonstrated in HPLC (*18*, *19*) and for microbore column separations (*20*). The high sensitivity of thermal lens detection could make it the OTLC detection method of choice for nonfluorescent compounds. In this paper we report the results of preliminary experiments demonstrating the feasibility of thermal lens detection for OTLC.

EXPERIMENTAL SECTION

Chromatography. The OTLC apparatus used in this work is shown in Figure 1. Capillary columns, 6–8 m × 20 μm i.d., were drawn from stock Pyrex glass tubes by using a glass drawing machine (Shimadzu, Model GDM-1, Kyoto, Japan). The inside surfaces of the columns were etched and bonded with dimethyloctadecylchlorosilane (ODS) using a procedure similar to that reported by Jorgenson and Guthrie (*4*). Five-nanoliter sample volumes were injected with an on-column injection procedure reported previously (*21*). Mobile phase was pumped through the columns at a linear velocity of approximately 0.5 cm/s with a Haskel (Burbank, CA), Model 27502, pneumatic amplifier pump.

Detection. Fluorescence detection was accomplished either on-column or in optical flow cells constructed from thin-wall, 100 μm i.d., capillary tubes (Vitro Dynamics, Rockway, NJ). The capillary tubes were epoxied into short pieces of needle gage stainless steel tubing. The stainless steel tubing served to protect the fragile flow cells during the connection procedure and also helped to match the outer diameter of the flow cell to that of the column (about 600 μm for the columns used in this work). The latter condition is important in assuring that there are no void spaces between the column and flow cell and to ensure that the column and flow cell openings are properly aligned. Thermal lens detection was accomplished with 100 or 200 μm square capillary tube flow cells, obtained from Vitro Dynamics, and connected to the columns by using the procedure described above. The flow cells were positioned in the focused laser beam by use of an optical fiber positioner. A short piece of narrow-bore capillary column was connected to the outlet of the flow cell to provide back pressure, thereby minimizing degassing problems.

The laser employed in our work was a Spectra Physics (Mountain View, CA) Model 171, argon ion laser, operated at 488 nm and 300 mW for the fluorescence work and at 458 nm and 500–800 mW for the thermal lens work. During fluorescence detection the laser radiation was focused into the flow cell with a 25 mm focal length lens or into the capillary column for on-column detection with a 19 mm focal length lens. A 25 mm diameter $f/1$ lens was used to collect the fluorescence emission and image it onto the entrance slit of a monochromator (Instruments SA, Metuchen, NJ, Model H 10). The monochromator was set to 540 nm and had a 16-nm band-pass. Signals were monitored with an RCA 1P28 photomultiplier tube (PMT) and a photometer (Gencom, Plainview, NY, Model 1012, picoammeter).

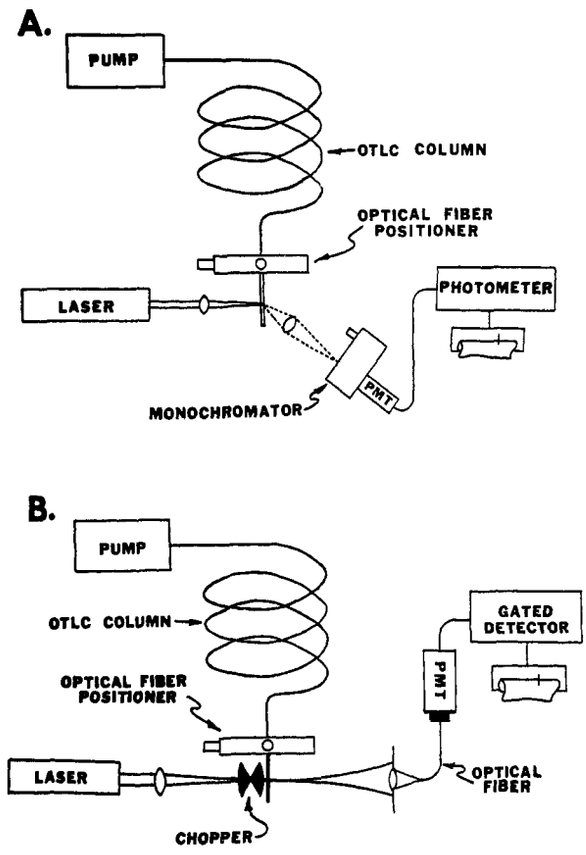

Figure 1. Block diagrams of fluorometric (A) and thermal lens (B) detectors for OTLC.

During thermal lens detection the laser radiation was focused into the 100- or 200-μm flow cells, perpendicular to a side, using 25 or 60 mm focal length lenses, respectively. The laser beam was modulated at 500 Hz with a mechanical chopper. The chopper was positioned in the path of the laser beam approximately 0.3 cm in front of the flow cell. The thermal "blooming" of the laser beam was monitored by placing in the path of the diverging beam, approximately 1 m from the flow cell, a 100 mm focal length, 20 mm diameter lens with an optical fiber at its focal point. The collected radiation was monitored with the PMT after suitable attenuation with neutral density filters.

The signal arising from this single beam thermal lens configuration was processed with a gated detector (Quanta-Ray, Mountain View, CA, Model DGA-1). The 100-μs gate duration of this detector was triggered by the synchronous output of the chopper. In order to adjust the time of the gating of the detector, relative to the exposure of the flow cell to the laser radiation, the chopper was spatially translated perpendicular to the laser beam. This permitted temporal inspection of the formation of the thermal lens.

Reagents. Fluorescence detection was performed by using as solutes several alkyl amines (Alltech Associates, Inc., amine analytical standard kit) derivatized with 7-chloro-4-nitrobenz-2,1,3-oxadiazole (NBD-Cl). The amines were derivatized by adding a weighed amount of amine to an acetonitrile solution containing approximately a 10-fold excess of NBD-Cl. The amine–NBD derivatives were separated on a 8.3 m × 20 μm i.d. column using a mobile phase that was 20% acetonitrile (HPLC grade) in water.

Table I. Typical OTLC Parameter Values

parameter	value
column length (L_c)	7.0 m
column diameter (d_c)	20 μm
diffusion coefficient (D_m)	1.0×10^{-5} cm²/s
flow velocity (v)	0.50 cm/s
capacity factor (k)	0.50

Preliminary thermal lens studies were performed in 200 μm square flow cells using alkaline, aqueous solutions of phenolphthalein. Thermal lens detection for actual OTLC separations was performed in 100 μm square flow cells using three nitroaniline compounds (*o*-nitroaniline, 4,5-dimethyl-2-nitroaniline, and *N*,*N*-dimethyl-3-nitroaniline). The nitroaniline compounds were obtained in reagent grade from Aldrich Chemicals. A 7.5 m × 20 μm i.d. column and a mobile phase that was 40% methanol (HPLC grade) in water were used to separate the nitroaniline compounds.

RESULTS AND DISCUSSION

Flow Cell Considerations. Equations 1 and 2 can be used to calculate the height equivalent to a theoretical plate, H_c, and plate number, N_c, for an open tubular column with, as is usually the case, negligible solute band dispersion due to both mass transfer in the stationary phase and the solute injection process.

$$H_c = \frac{2D_m}{v} + \frac{1 + 6k' + 11k'^2}{(1 + k')^2} \frac{d_c^2 v}{96 D_m} \quad (1)$$

$$N_c = L_c/H_c \quad (2)$$

The first and second terms in eq 1 represent, respectively, the contributions of axial diffusion in the mobile phase and resistance to mass transfer in the mobile phase to the dispersion of solute bands. When the parameter values typical of the experiments reported herein, and listed in Table I, are inserted into these equations, a column efficiency of 110 000 theoretical plates is calculated.

The variance of a solute band in volume units, resulting from dispersion in the column, $\sigma_{v,c}^2$, can be calculated by using

$$\sigma_{v,c}^2 = V_R^2/N_c \quad (3)$$

where V_R is the retention volume of the solute. For the parameter values given previously, eq 3 yields a variance of 100 nL² or total peak volume (4σ) of 40 nL. It is obvious from these calculations that it is possible to obtain exceptional column performance in OTLC, but only if a detector is employed which does not disperse narrow solute bands.

On-column fluorescence detection has been utilized in OTLC (*4*). There are two principal advantages in this type of detection. First, since there is no flow cell, there is no band dispersion due to the detector, providing the effective illuminated volume of the column is much smaller than the smallest solute band volume and the detector response time is sufficiently short. Second, the high sensitivity of fluorometric detection permits detection of very small injection quantities.

We have utilized on-column, laser fluorometric detection in evaluating the OTLC columns prepared in this work. We have also compared laser fluorometric detection in flow cells to on-column detection, in order to assess the contribution of the flow cells to solute band variances. This evaluation is important since the utility of on-column optical detection is limited by the composition and geometry of most OTLC columns. The materials which have been most successfully employed in the preparation of bonded-phase columns (e.g., soft and borosilicate glasses) contain impurities which absorb UV radiation and fluoresce. With these column materials, on-column detection is restricted to the near-UV and visible region of the spectrum. Moreover, the large wall thickness and narrow inner diameter of most OTLC columns make it difficult to efficiently focus the incident laser radiation into or through the column. This is especially important in thermal lens detection. The Gaussian intensity profile of the laser beam must be maintained at the column (or flow cell) and in the far field.

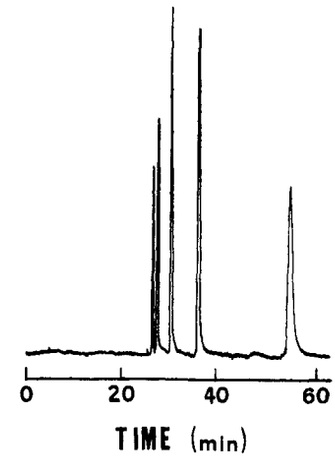

Figure 2. OTLC separation of amine–NBD derivatives, using on-column fluorescence detection. The derivatives in order of elution are ethylamine, *n*-propylamine, *n*-butylamine, cyclohexylamine, and *n*-hexylamine.

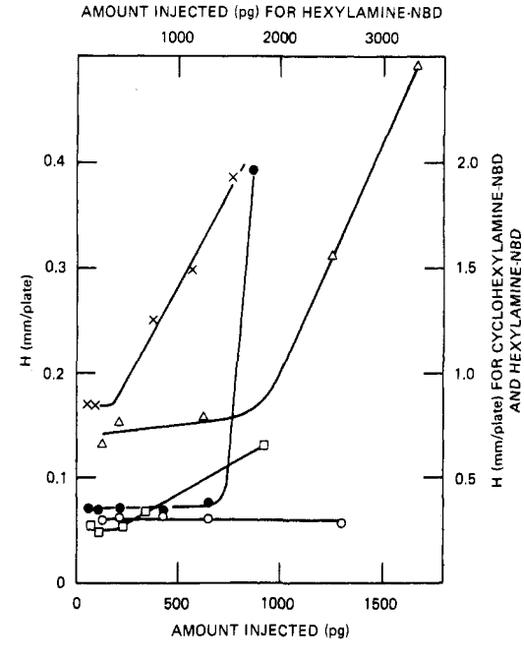

Figure 3. Relationship between plate height and amount of sample injected for a mixture of amine–NBD derivatives. A 20 μm i.d. × 8.6 m, ODS bonded-phase column and a 23% acetonitrile in water mobile phase were employed. The mixture was ethylamine (○), propylamine (●), *n*-butylamine (×), cyclohexylamine (□), and *n*-hexylamine (△).

A chromatogram illustrating the efficiency of the OTLC columns prepared in this work and the sensitivity of laser fluorometric detection is shown in Figure 2. This chromatogram was obtained by using a 8.3 m × 20 μm i.d., ODS bonded-phase column and employing on-column detection. The mobile phase was 20% acetonitrile in water. Minimum detectable injected quantities of the separated amine–NBD derivatives were in the low picogram range. Figure 3 illustrates the importance of employing sensitive detectors in OTLC. The figure contains a plot of plate height vs. amount injected for a five-component mixture of amine–NBD derivatives. For some of the derivatives, increases in plate height due to column

Table II. Effect of Flow Cells on Solute Band Variances

	solute band variance, nL^2		
		flow cell contribution	
flow cell	obsd	exptl	calcd
on-column	41		
100 μm round	66	25	0.001
100 μm square	97	56	0.060

overload occur at injected amounts less than 1 ng. The required sensitivity is possible with fluorometric detection. While this is the first reported use of laser fluorometric detection in OTLC, the focus of this work has been the development of the potentially more versatile thermal lens detection for OTLC.

Initial attempts at on-column thermal lens detection were unsuccessful due to a severe distortion of the Gaussian laser beam profile after passing through the column. Better far-field beam profiles were observed when thin-walled round flow cells were employed. However, the best beam profiles were observed with square flow cells. A study was initiated to determine the magnitude of the contributions of these flow cells to solute band variance.

The fluorescence peak profiles of ethylamine–NBD were obtained for 100 μm i.d. round and 100 μm inner dimension square flow cells, which were used with a 20 μm i.d. open tubular column. The observed solute band variances appear in Table II. The experimental flow cell contributions to the observed variances were determined as the difference between the observed variances obtained by using the flow cells and the observed variance for on-column detection. The theoretical values for the flow cell contributions to the variance, $\sigma_{v,d}^2$, were calculated by using

$$\sigma_{v,d}^2 = H_d L_d \tag{4}$$

where L_d is the length of flow cell up to illuminated spot and H_d is the detector (i.e., flow cell) plate height. H_d for the round flow cell was calculated by using eq 1 with the flow cell values of flow velocity, diameter, and capacity factor ($k' = 0$) inserted, and H_d for the square flow cell was calculated by using a similar expression derived by Golay for rectangular columns with end effects (*22*). The value of D_m for these flow cell plate height calculations was determined by using eq 1 and the on-column detection results.

Changing the position of the illuminated spot along the length of the flow cell did not have a noticeable effect on the observed solute band variances. Thus we concluded that the very large difference between the experimental and theoretical contributions of the flow cells to the solute band variances is probably due to dispersion occurring at the column-flow cell connection. The theoretical expressions used to calculate the flow cell plate height assume a parabolic flow profile. The sudden jump in size and shape of the flow channel upon entering the flow cell results in a region of nonuniform flow, as well as regions in the corners of the flow cell which are poorly swept or stagnant. The possibility of gaps between the column and the flow cell also exists. All of these factors could contribute to the dispersion of solute bands. It may be possible to eliminate or at least minimize the band dispersion occurring at the column-flow cell connection by employing tapered flow cells. These flow cells would have an inner dimension at their inlet which matches that of the column and then gradually increase in their inner dimension. This approach to flow cell design is currently under investigation in our laboratories.

Proper optical alignment is more difficult to achieve for optical detection in OTLC than it is for larger scale liquid chromatography. In the case of thermal lens detection the focused beam waist, ω_0, of the Gaussian laser beam must be several times smaller than the inner dimension of the flow cell while the confocal parameter, Z_c (the distance at the beam waist over which the focused beam is roughly collimated), should be considerably larger than the optical path dimension of the flow cell. The beam waist for a focused Gaussian laser beam can be calculated from the beam waist, $\omega_{0,l}$, and confocal parameter, $Z_{c,l}$, of the laser by using

$$\omega_0^2 = \frac{\omega_{0,l}^2}{(Z_{c,l}/f)^2 + (1 - Z_l/f)^2}$$

where Z_l is the distance from the laser beam waist to the focusing lens and f is the focal length of the focusing lens. Shorter focal length lenses yield smaller beam waist values. By use of information supplied by the laser manufacturer, the calculated values for the 60 mm and 25 mm focal length lenses employed in this thermal lens work are 8.0 μm and 2.6 μm, respectively.

The confocal parameters for these beam waist values can be calculated by using

$$Z_c = \pi\omega_0^2/\lambda \tag{6}$$

where λ is the wavelength of the radiation. Equations 5 and 6 point out the importance of choosing the proper lens for the flow cell employed. Unfortunately, eq 5 does not consider the effect of spherical aberration of the lens and the actual beam waist is expected to be larger than that calculated by the equation. Nevertheless, the equations are a good starting point in choosing a suitable lens and lens position. Subsequent adjustments of the lens focal length and position may be necessary in order to achieve a clean focusing of the laser radiation through the flow cell.

Thermal Lens Detection. Absorbance detection is used much more often in liquid chromatography than fluorescence detection due to its fairly universal response. However, conventional absorbance detection does not generally possess the sensitivity required for detection in OTLC. The enhancement in sensitivity of thermal lens detection over the conventional absorbance technique offers the opportunity to detect smaller injected solute amounts in shorter optical path length flow cells.

With the parabolic thermal lens model (*23*), the signal arising from an experimental arrangement such as was used in this work is described by

$$I_{(t)} = I_{(0)}\left[1 + \frac{2.3EA}{1 + t_c/2t}\,\frac{2Z_1Z_c}{Z_1^2 + Z_c^2} + \left(\frac{2.3EA}{1 + t_c/2t}\right)^2 \frac{Z_1Z_c}{Z_1^2 + Z_c^2}\right]^{-1} \tag{7}$$

where $I_{(t)}$ is the intensity measured at time t following the initiation of the thermal lens, E is the enhancement of the measurement relative to Beer's law, A is the absorbance, t_c is the time constant for the formation of the thermal lens, and Z_1 is the distance from the sample cell to the focused laser beam waist. The relevance of the terms appearing in eq 7 as they pertain to detection in OTLC will be discussed.

Of considerable interest to thermal lens detection in chromatography is the effect of flow on the thermal lens signal. Under flow conditions encountered in HPLC it has been demonstrated that small reductions in thermal lens enhancement factors are observed (*24*). For the flow cell flow velocities employed in this OTLC work (approximately 0.02 cm/s) no reductions, relative to stagnant solution measurements, were observed. However, with the column removed

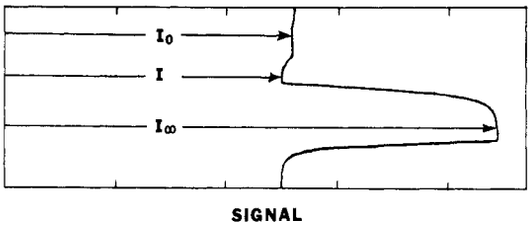

Figure 4. Thermal lens and conventional Beer's law absorbance signals for a flowing sample illustrating the enhancement afforded by thermal lens detection.

it was possible to operate at flow velocities (greater than approximately 10 cm/s) for which no thermal lens signal could be detected.

The enhancement, E, of the thermal lens signal relative to Beer's law is dependent on a number of experimental parameters which can be manipulated, to a degree, when performing thermal lens detection in OTLC. Increasing laser power and decreasing wavelength lead to larger enhancements. The former is limited by the maximum power of the laser, while the latter is restricted to the absorption bands of the solute of interest. The thermooptical properties of the solvent also influence the magnitude of the enhancement. Solvents with a low polarity generally have properties which yield the largest enhancements. Unfortunately, the bonded, reverse-phase OTLC columns employed in this work require very polar mobile phases. There is a strong motivation to develop bonded, normal-phase columns, so as to permit the use of low polarity mobile phases which would exhibit large enhancements.

Figure 4 illustrates the enhancement offered by the thermal lens effect over conventional absorbance detection for a flowing sample. The apparatus shown in Figure 1B was employed in this experiment except that the column was replaced by a section of relatively wide-bore tubing. The chopper was positioned so that the gate delay was relatively long and appropriate to observe the steady-state thermal lens signal (I_∞). A 60 mm focal length focusing lens was used in the experiment. A 200 μm square flow cell and the connective tubing were filled with an alkaline, aqueous solution, and the pump was filled with a 1 μM phenolphthalein in alkaline, aqueous solution. The laser was operated at 515 nm and a power at the flow cell of 0.4 W. I_0 in Figure 4 is the signal intensity for the alkaline, aqueous solution at a very fast flow rate, I is the signal resulting from the arrival of the phenolphthalein solution in the flow cell, and I_∞ is the signal resulting from the same phenolphthalein solution when the flow rate has been decreased to a value compatible with OTLC. Taking the case for fast flow to be a measurement without a thermal lens effect, there exists a situation which is equivalent to Beer's law absorption. For the slow flow case, the system response is enhanced. The increase in intensity, rather than a decrease, is a result of the placement of the flow cell before the beam waist of the focused laser beam. This corresponds to a negative value of Z_1 which produces a value of $I_{(t)}$ which is greater than I_0, or a decrease in the far-field beam spot size due to the thermal lens. Placing the flow cell after the beam waist has the opposite effect.

On the basis of the molar absorptivity and concentration of the phenolphthalein solution, the response at fast flow roughly corresponds with Beers law. The slow flow, a thermal lens situation, provides an enhancement of approximately 20 over the Beers law measurement. While this is slightly less than half the calculated enhancement for water of 0.11/mW (*23*), very little effort was made to optimize the critical position of the flow cell in the focused laser beam (see below). This experiment clearly illustrates the ability to observe large thermal lens enhancements under conditions which are compatible with OTLC detection.

The time constant, t_c, for the formation of a thermal lens is given by

$$t_c = \frac{\omega^2 \rho C_p}{4k} \tag{8}$$

where ρ, C_p, and k are the density, specific heat, and thermal conductivity, respectively, of the sample and ω is the beam waist at the sample cell. The experimental arrangement and phenolphthalein solution used to obtain the data for Figure 4 were also used to measure t_c. By translating the chopper perpendicular to the laser beam it is possible to observe the transient thermal lens signal. Fitting the observed transient signal to eq 7 yielded a t_c value of 0.26 ms. However, the relatively large gate duration of the gated detector made it impossible to observe the very early stages of the thermal lens formation and this limited the accuracy of the t_c determination. The value of t_c for these experimental conditions can also be calculated by using eq 8. Using the previously calculated beam waist for the 60 mm focal length lens, and assuming the flow cell was positioned one confocal parameter from the beam waist, the value of ω for the calculation is 11 μm (*23*). Inserting ω and the solvent parameters into eq 8 results in a calculated value of t_c of 0.21 ms. Considering the limitations of the method used to obtain the experimental value of t_c and the tendency of eq 5 to predict erroneously small beam waist values, the agreement between the observed and calculated values is reasonable.

The very short time constants for thermal lens detection in OTLC influence the proper choice of signal recovery instrumentation. The analytical advantages of a kinetic approach to monitoring signals for single beam thermal lens arrangements have been reported (*25*). This approach would be more difficult for detection in OTLC since it would require very fast analog to digital conversions of the rapidly changing signal intensity. However, there are advantages inherent to the shorter time constants. For example, shorter time constants can reduce the sensitivity of the thermal lens to flow (*26*). Double beam thermal lens instruments employ either a chopped continuous wave laser or a pulsed laser to create a thermal lens in a sample. A lock-in amplifier is generally used to monitor the modulated signal from a second continuous wave laser, which probes the thermal lens. This approach, using high modulation frequencies in order to accommodate the root mean square signal response of a lock-in amplifier, should be feasible for detection in OTLC.

The gated detector used in this work was obtained with the eventual goal of using a pulsed, double beam arrangement for thermal lens detection in OTLC. It was not well-suited to recover thermal lens signals for the single beam arrangement employed in these preliminary studies. The gated detector was used to measure $I_{(t)}$ at a time which was fairly long compared to t_c. In this mode of operation the detector is very susceptible to noise resulting from changes in the position and intensity of the laser beam. Less noise is expected for future, pulsed, double beam experiments since the gated detector can be arranged to subtract the pregate (no thermal lens) signal from the gate signal. This should provide some correction for changes in the position of the laser beam. In addition, the gated detector has a reference channel which can be used to normalize signals to the pulse energy of the heating laser.

The position dependence of the thermal lens signal can be discerned from eq 7. The equation predicts an optimum signal when the sample cell is positioned one confocal parameter before or after the focused laser beam waist. The aberrant theoretical model of the thermal lens effect predicts an optimum when Z_1 is equal to $3^{1/2}\, Z_c$ (*17*). The tight focusing that is necessary for thermal lens detection in OTLC results in small confocal parameters. This makes flow cell positioning

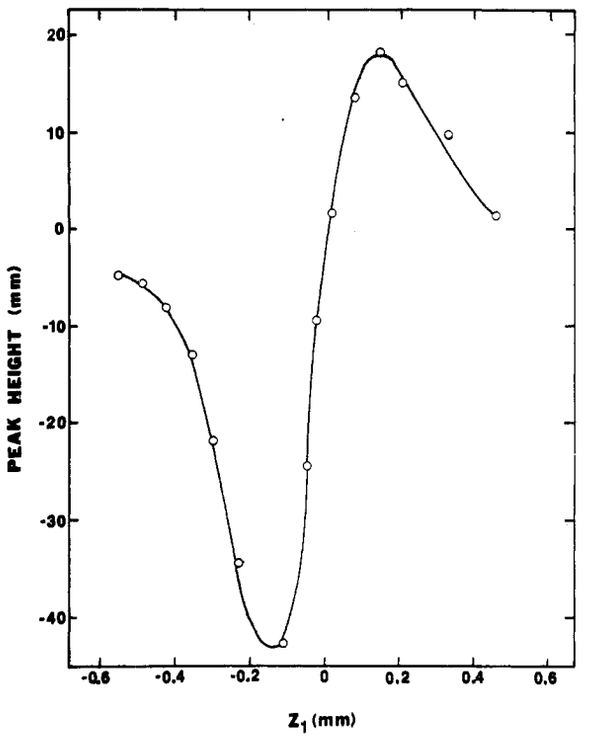

Figure 5. Positional dependence of the thermal lens signal for detection in OTLC.

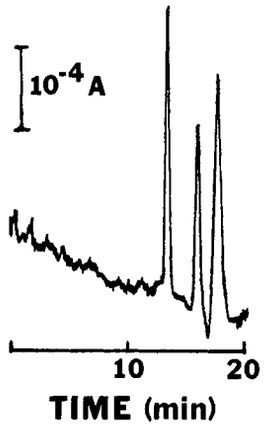

Figure 6. OTLC separation of nitroaniline compounds using thermal lens detection. The compounds in order of elution are *o*-nitroaniline, 4,5-dimethyl-2-nitroaniline, and *N*,*N*-dimethyl-3-nitroaniline.

very critical. A plot of peak height vs. Z_1 for injections of an *o*-nitroaniline solution is shown in Figure 5. Optimum signals occur for Z_1 values of 0.15 mm. This study was performed with a 20 μm i.d. column, a 100 μm square flow cell, and a 25 mm focal length lens. Assuming accurate models and using eq 6, the optimum flow cell position indicates that the beam waist for the experiment was 4.7 μm for the parabolic lens model and 3.6 μm for the aberrant lens model. With laser resonator parameters, eq 5 yielded a beam waist of 2.6 μm. Considering the limitations of eq 5 cited earlier, the agreement is reasonable.

Figure 5 also shows larger signals when the flow cell is positioned before the beam waist. This is contrary to predictions based on eq 7 and previously reported thermal lens studies in large sample cells. However, the theoretical model used in deriving eq 7 assumes a thin thermal lens (i.e., path length $<< Z_c$). This assumption is not valid for our work with very small flow cells.

Figure 6 illustrates a chromatogram of nitroaniline compounds separated by OTLC with thermal lens detection. A 7.5 m × 20 μm i.d., ODS bonded-phase column and a mobile phase that was 40% methanol in water were used for the separation. The peaks correspond to 410 pg of *o*-nitroaniline, 310 pg of 4,5-dimethyl-2-nitroaniline, and 3.6 ng of *N*,*N*-dimethyl-3-nitroaniline. The base line noise level for this chromatogram is approximately 3×10^{-5} absorbance units. A calibration plot for the *o*-nitroaniline yielded a LOD of 30 pg ($S/N = 2$) and a linear regression constant of 0.994 from the LOD to 1.2 ng injected. We believe these preliminary studies demonstrate the potential of thermal lens detection for providing the sensitivity, low solute band dispersion, and universal response needed for the efficient utilization of OTLC in organic analysis.

Registry No. Ethylamine, 75-04-7; *n*-propylamine, 107-10-8; *n*-butylamine, 109-73-9; cyclohexylamine, 108-91-8; *n*-hexylamine, 111-26-2; *o*-nitroaniline, 88-74-4; 4,5-dimethyl-2-nitroaniline, 6972-71-0; *N*,*N*-dimethyl-3-nitroaniline, 619-31-8.

LITERATURE CITED

(1) Knox, J. H.; Gilbert, M. T. *J. Chromatogr.* **1979**, *186*, 405–418.
(2) Yang, F. J. *J. Chromatogr. Sci.* **1982**, *20*, 241–251.
(3) Guiochon, G. *Anal. Chem.* **1981**, *53*, 1318–1325.
(4) Jorgenson, J. W.; Guthrie, E. J. *J. Chromatogr.* **1983**, *225*, 335–348.
(5) Tsuda, T.; Katsuyoshi, T.; Nakagawa, G. *J. Chromatogr.* **1981**, *214*, 283–290.
(6) Slais, K.; Krejci, M. *J. Chromatogr.* **1982**, *235*, 21–19.
(7) Tijssen, R.; Bleumer, J. P. A.; Smit, A. L. C.; Van Kreveld, M. E. *J. Chromatogr.* **1981**, *218*, 137–165.
(8) McGuffin, V. L.; Novotny, M. *Anal. Chem.* **1981**, *53*, 946–951.
(9) Krejci, M.; Tesarik, K.; Pajurek, J. *J. Chromatogr.* **1980**, *191*, 17–23.
(10) Yang, F. J. *HRC CC, J. High Resolut. Chromatogr. Chromatogr. Commun.* **1981**, *4*, 83–85.
(11) Yang, F. J. *HRC CC, J. High Resolut. Chromatogr. Chromatogr. Commun.* **1981**, *3*, 589–590.
(12) Hibi, K.; Ishii, D.; Fujishima; Takeuchi, T.; Nakanishi, T. *HRC CC, J. High. Resolut. Chromatogr. Chromatogr. Commun.* **1978**, *7*, 21–27.
(13) Novotny, M. *Anal. Chem.* **1981**, *53*, 1294A–1308A.
(14) Yeung, E. S.; Sepaniak, M. J. *Anal. Chem.* **1980**, *52*, 1465A–1475A.
(15) Folestad, S.; Johnson, L.; Josefsson, B. *Anal. Chem.* **1982**, *54*, 925–929.
(16) Dovichi, N. J.; Harris J. M. *Anal. Chem.* **1979**, *51*, 728–732.
(17) Sheldon, S. J.; Knight, L. V.; Thorne, J. M. *Appl. Opt.* **1982**, *21*, 1663–1669.
(18) Leach, R. A.; Harris, J. M. *J. Chromatogr.* **1981**, *218*, 15–19.
(19) Buffet, C. E.; Morris, M. D. *Anal. Chem.* **1982**, *54*, 1824–1825.
(20) Buffet, C. E.; Morris M. D. *Anal. Chem.* **1983**, *55*, 376–378.
(21) Maskarinec, M. P.; Vargo, J. D.; Sepaniak, M. J. *J. Chromatogr.* **1983**, *261*, 245–251.
(22) Golay, M. J. E. *J. Chromatogr.* **1981**, *216*, 1–8.
(23) Harris, J. M.; Dovichi, N. J. *Anal. Chem.* **1980**, *52*, 695A–706A.
(24) Dovichi, N. J.; Harris, J. M. *Anal. Chem.* **1981**, *53*, 689–692.
(25) Dovichi, N. J.; Harris, J. M. *Anal. Chem.* **1981**, *53*, 106–109.
(26) Carter, C. A.; Harris, J. M. *Anal. Chem.*, in press.

RECEIVED for review November 17, 1983. Accepted February 23, 1984. This research was sponsored by the Office of Health and Environmental Research, U.S. Department of Energy, under Contract W-7405-eng-26 with the Union Carbide Corp. and the Division of Chemical Sciences, Office of Basic Energy Sciences, U.S. Department of Energy, under Contract DEAS05-83ER13127 with the University of Tennessee (Knoxville).